Pinning and trapped field in MgB$_2$- and MT-YBaCuO bulk superconductors manufactured under pressure

You may also be interested in:

Observation of strong intrinsic pinning in MgB2 films
Soon-Gil Jung, N H Lee, W K Seong et al.

Pinning and trapped field in MgB₂- and MT-YBaCuO bulk superconductors manufactured under pressure

T Prikhna[1,12], **M Eisterer**[2], **X Chaud**[3], **H W Weber**[2], **T Habisreuther**[4],
V Moshchil[1], **A Kozyrev**[1], **A Shapovalov**[1], **W Gawalek**[5], **M Wu**[5], **D Litzkendorf**[4],
W Goldacker[6], **V Sokolovsky**[7], **V Shaternik**[8], **J Rabier**[9], **A Joulain**[9],
G Grechnev`[10], **V Boutko**[11], **A Gusev**[11], **A Shaternik**[1], **P Barvitskiy**[1]

[1] V. Bakul Institute for Superhard Materials of the National Academy of Sciences of Ukraine, 2, Avtozavodskaya Str., Kiev 07074, Ukraine

[2] Atominstitut, Vienna University of Technology, Stadionallee 2, 1020 Vienna, Austria

[3] Laboratoire National des Champs Magnétiques Intenses (LNCMI/CNRS), 25 Avenue des Martyrs, BP 166, 38042 Grenoble Cedex 9, France

[4] Leibniz-Institut für Photonische Technologien, Albert-Einstein-Straße 9, 07745 Jena, Germany

[5] Magnetworld AG, Buchaer Straße 6, 07745 Jena, Germany

[6] Karlsruhe Institute of Technology (KIT), 76344 Eggenstein, Germany

[7] Ben-Gurion University of the Negev, P.O.B. 653, Beer-Sheva 84105, Israel

[8] G.V. Kurdyumov Institute for Metal Physics of the National Academy of Sciences of Ukraine, 03680 Kyiv, Ukraine

[9] Institute P', PHYMAT, UMR 6630, CNRS Université de Poitiers, SP2MI, BP 30179, F-86 962 Futuroscope, France

[10] B. Verkin Institute for Low Temperature Physics of the National Academy of Sciences of Ukraine, Kharkov 61103, Ukraine

[11] Donetsk Institute for Physics and Engineering named after O.O. Galkin of the National Academy of Sciences of Ukraine, R. Luxemburg str.72, Donetsk-114, 83114, Ukraine

E-mail: [1] prikhna@mail.ru, [2] eisterer@ati.ac.at, [3] tobias.habisreuther@ipht-jena.de, [4] xavier.chaud@lncmi.cnrs.fr, [5] wuminzhi@aol.com, [6] wilfried.goldacker@kit.edu, [7] sokolovv@bgu.ac.il, [8] shaternik@mail.ru, δ[9] jacques.rabier@univ-poitiers.fr, [10] grechnev@ilt.kharkov.ua, [11] boutko@teor.fti.ac.donetsk.ua

Abstract. The relevant pinning centers of Abrikosov vortices in MgB₂–based materials are oxygen-enriched Mg-B-O inclusions or nanolayers and inclusions of MgB_x (x>4) phases. The high critical current densities, j_c, of 10^6 and $10^3 A/cm^2$ at 1 and 8.5 T, respectively, at 20 K can be achieved in polycrystalline materials (prepared at 2 GPa) containing a large amount of admixed oxygen. Besides, oxygen can be incorporated into the MgB₂ structure in small amounts ($MgB_{1.5}O_{0.5}$), which is supported by Auger studies and calculations of the DOS and the binding energy. The j_c of melt textured YBa₂Cu₃O₇₋δ (or Y123)-based superconductors (MT-YBaCuO) depends not only on the perfectness of texture and the amount of oxygen in the

---

[12] To whom any correspondence should be addressed.

Y123 structure, but also on the density of twins and micro-cracks formed during the oxygenation (due to shrinking of the *c*-lattice parameter). The density of twins and micro-cracks increases with the reduction of the distance between Y_2BaCuO_5 (Y211) inclusions in Y123. At 77 K j_c=8·10^4 A/cm^2 in self-field and j_c=10^3 A/cm^2 at 10 T were found in materials oxygenated at 16 MPa for 3 days with a density of twins of 22–35 per μm (thickness of the lamellae: 45-30 nm) and a density of micro-cracks of 200–280 per mm. Pinning can occur at the points of intersection between the Y123 twin planes and the Y211 inclusions. MT-YBaCuO at 77 K can trap 1.4 T (38×38×17 mm, oxygenated at 0.1 MPa for 20 days) and 0.8 T (16 mm in diameter and 10 mm thick with 0.45 mm holes oxygenated at 10 MPa for 53 h). The sensitivity of MgB_2 to magnetic field variations (flux jumps) complicates estimates of the trapped field. At 20 K 1.8 T was found for a block of 30 mm in diameter and a thickness of 7.5 mm and 1.5 T (if the magnetic field was increased at a rate of 0.1 T) for a ring with dimensions 24×18 mm and a thickness of 8 mm.

1. Introduction

Both MgB_2- and MT-YBaCuO bulk materials are good candidates for the same cryogenic applications. The working temperature of MT-YBaCuO can be higher (77 K) than that of MgB_2 (20-30 K), while MgB_2-based materials are much cheaper and easier to prepare. Excellent superconductive and mechanical characteristics and well developed manufacturing technologies make these materials extremely promising for fault current limiters (FCL), electrical machines, for screening magnetic and gravitation fields, for magnetic bearings, contactless mixers, as magnets for magnetron sputtering, for MAGLEV transportation (particularly in clean rooms) and other devices based on the principle of levitation, etc.

The manufacturing technologies for the preparation of superconducting materials with high critical current densities, j_c, are very different for MgB_2 and MT-YBaCuO due to the difference of their coherence lengths. The comparatively large coherence length of MgB_2 allows attaining high critical currents in polycrystalline materials, because the grain boundaries contribute to pinning. Therefore, the synthesis technologies aim at the formation of dense nanostructural MgB_2–based materials with long lengths of grain boundaries. Hot pressure (at 30 MPa), spark plasma or SPS (at 50 MPa) and high pressure (2 GPa) synthesis allow attaining j_c of around 4·10^5 - 10^6 A/cm^2 at 20 K in a 1 T field [1, 2] and high trapped fields [3].

In polycrystalline $YBa_2Cu_3O_{7-\delta}$ (Y123) the grain boundaries (even the misalignment of grains by more than 5 degrees) are obstacles for the superconducting current flow because of the small coherence length of the compound, which makes it impossible to attain j_c above 10^3 A/cm^2 at 77 K in self-field. Therefore, technologies of melt textured growth on seed crystals were developed (i.e. the formation of a pseudo-single crystalline Y123 structure with a high density of small non superconducting inclusions of the Y_2BaCuO_5 (Y211) phase), which allow attaining j_c in self-field above 6·10^4 A/cm^2 in MT-YBaCuO at 77 K and trapped fields of around 1 T (depending on the size of the pellets) [4-7].

Because of the difference in coherence length, the size of the inhomogeneities which can act as pinning centers in bulk MgB_2-based materials and in MT-YBaCuO, are different (they should be comparable to the coherence length). Thus in Y123 twins, dislocations, stacking faults, and possibly micro-cracks (formed because of shrinking of *c*-parameter of Y123 during oxygenation) [4, 8-10] can be responsible for pinning, whereas in MgB_2 grain boundaries of nano-grains of the matrix phase (with a stoichiometry close to MgB_2), nanosized inclusions of MgO, Mg-B-O and higher magnesium borides MgB_x(x≥4) or inclusions of other secondary phases can act as pinning centers [11-13]. In MT-NEG123 (or Nd-Eu-Gd-Ba-Cu-O-based melt-textured materials) an array of nanolamellas within regular twins has been proposed as pinning centers responsible for very high irreversibility fields [14]. The distance between the nanolamellas was only several nanometers. The nanolamellas inside the twins were not observed when the amount of NEG211 in MT-NEG123 increased above 10 mol.%, which was accompanied with the reduction of the irreversibility field.

It is well known that for attaining high transition temperatures and critical current densities in $YBa_2Cu_3O_{7-\delta}$ the concentration of oxygen $(7-\delta)$ in the unit cell and its distribution in the basal planes are very important (the formation of oxygen chains in the basal planes and an amount of oxygen $7-\delta\sim6.9\text{-}7.0$ are optimal) [8, 15]. For the preparation of MT-YBaCuO with good superconducting properties the oxygenation stage (usually a separate process) is essential, which is needed in order to transform the non superconducting $YBa_2Cu_3O_{7-\delta}$ matrix phase of MT-YBaCuO with $7-\delta\sim6.3\text{-}6.4$ into the superconducting phase with $7-\delta\sim6.9\text{-}7.0$. During the oxygenation process twins, dislocations, stacking faults, micro- and macro-cracks are formed, because the oxygen incorporation into the $YBa_2Cu_3O_{7-\delta}$ structure is accompanied by a shrinking c-axis lattice parameter.

Although MgB_2 is nominally an oxygen free compound, admixed oxygen is usually present, even if high purity initial ingredients are used and the preparation is conducted under protective atmosphere.

Our results support the conclusion that excellent SC properties (critical current density and thus trapped magnetic field) of MT-YBaCuO are connected to a high extent with a high density of twins, which can be influenced by pressure-temperature conditions during the oxygenation process and by the density and homogeneous distribution of Y211 inclusions formed during melt-texturing (which, in turn, even depend on the kind of initial ingredients). The superconducting performance of MgB_2-based materials essentially depends on the distribution of admixed oxygen in the form of Mg-B-O nanoinclusions or nanolayers (with most probably MgO structure) and on the amount of oxygen dissolved in the hexagonal superconducting matrix, which can be regulated by the temperature – pressure conditions during manufacturing and by additions, such as Ti and SiC, for example. The solution of some oxygen in the superconducting MgB_2 structure does not contradict its SC performance according to the calculated density of states and the binding energy. Furthermore, it was shown that the level of trapped fields in bulk MgB_2 depends to a high extent on the penetration rate of the external magnetic field into the material, because too high rates provoke flux jumps leading to a destruction of the trapped magnetic field.

2. Experimental

In this study, three types of MT–YBCO initial ceramic samples were used: (type 1) - the traditional bulk MT–YBaCuO ceramic prepared according to the technology described in [6]. As the initial material a mixture of powdered $YBa_2Cu_3O_{7-\delta}$ (produced by Solvay Company), Y_2O_3, and CeO_2 in the ratio of $Y_{1.5}Ba_2Cu_3O_{7-\delta} + 1\%$ CeO_2 was used. The powders were thoroughly mixed and uniaxially compacted as square blocks with dimensions $40\times40\times20$ mm^3. Then a $SmBa_2Cu_3O_x$ seed crystal was placed onto the upper surface of each block and a modified process of melt texturing of a batch of 16–30 samples was performed under quasi-isothermal conditions in a furnace with six-sector heating capability. After melt-texturing, due to shrinking and after cutting off the bottom, the sample dimensions were $38\times38\times17$ mm^3. Texturing and cooling after texturing were carried out in air. Melt-textured ceramics of type 2 were prepared without and with small parallel holes (to reduce the depth into which oxygen could penetrate during oxygenation). The thin-wall MT-YBaCuO ceramics with holes do not contain pores and macro-cracks. MT-YBaCuO materials of type 2 (thin-walled and traditional) were prepared as described in [16] using $SmBa_2Cu_3O_x$ seed crystals (after finishing the texturing process air was slowly substituted by nitrogen; the samples were cooled from about 940 °C in nitrogen with a residual oxygen pressure below 5 mbar to avoid oxygen uptake and limit cracking due to oxygenation). Bulks with a diameter of about 20 mm with small parallel holes about 0.7 and 0.5 mm in diameter and with 1.2 or 2.5 mm spacing between each other were formed from the initial mixture, which contained 70 $YBa_2Cu_3O_{7-\delta}$, 30 Y_2BaCuO_5, and 0.15 PtO_2 wt %. After melt-texturing, the pellet had a diameter of 16 mm and the holes had a reduced diameter of about 0.6 mm and 0.45 mm. The top and bottom parts were cut and polished. The final thickness was about 10 mm. The holes did not prevent the growth of a single-domain structure from the seed crystal surface within the whole volume of a sample.

In this study, the initial ceramic blocks of types (1 and 2) were cut into rectangular parallelepipeds

Table1. Characteristics of initial boron powders

Type of amorphous boron (producer)	N ; wt %	C, wt %	H, wt %	O, wt %	average grain size
B(I) (H.C. Starck)	0.48	0.31	0.32	0.66	<5 µm
B(II) (HyperTech, USA)	1.02	3.5	0.87	-	<1 µm
B(III) (H.C. Starck)	0.40	0.47	0.37	1.5	4.0 µm
B(IV) (MaTeck 95-97%)	0.43	0.27	0.11	1.9	1.4 µm

measuring 3–4×3–4×5–8 mm in such way that the c crystallographic axis of Y123 was parallel to the longer side of parallelepipeds and the ab–plane parallel to the shorter dimensions. These sizes are suitable for placing the samples into a vibrating sample magnetometer for j_c measurements, which were performed in two perpendicular directions. The small samples were oxygenated together with the big ones, which were used for the trapped field measurements. The phase composition and the crystallographic structures were studied at room temperature by x-ray powder diffraction using a Philips X'pert'' and a DRON-3 diffractometer. The x-ray patterns were taken in an angular range of $2\Theta = 20$–$70°$ at a rate of 5 deg/min. The sample structure was studied using polarized light and transmission electron microscopes.

The bulk MgB_2 materials were synthesized from Mg and B taken in Mg:2B stoichiometry at 2 GPa quasi-hydrostatic pressure and at 600 - 1050 ^oC for 1 h (in contact with BN). We used Mg turnings Technical Specification of Ukraine 48-10-93-88 (designated as Mg(I)) or fine Mg powder produced by HyperTech, USA (designated as Mg(II)) and commercially available amorphous precursor B powders (Table 1). B and Mg were milled in a high-speed planetary activator with steel balls for 1-3 min.

Thin MgB_2 films were deposited by DC magnetron sputtering under 1 Pa Ar pressure on 8×8×0.2 mm^3 sized sapphire substrates in (0001) orientation at room temperature and subsequently annealed at 600-650 ^oC for 5 min in Ar under 10 Pa. For deposition we used an MgB_2 target synthesized by hot pressing at 30 MPa, 800 ^oC, 1 h using boron B(II).

The microstructure of the materials was characterized by x-ray structure analysis (with Rietveld refinement) and by SEM with microprobe x-ray and Auger (JAMP−9500F) analysis. The Auger spectroscope JAMP−9500F is combined in the same device with a high resolution SEM. It is possible to change the SEM microprobe analyzer for the Auger probe and to perform etching by Ar ions of the $1×1$ mm^2 analyzed material surface area. JAMP−9500F offers the possibility to quantitatively analyze small volumes of about 10 nm in diameter and 1 nm in depth. Thus, non-oxidized MgB_2 surfaces can be analyzed as well as the composition of nano-inclusions and nano-layers.

The critical current density, j_c, was estimated from magnetization measurements in an Oxford Instruments 3001 vibrating sample magnetometer (VSM) using the Bean model. The connectivity was estimated from the difference in resistivity at 40 K and 300 K measured by the four probe technique. The amount of the SC shielding fraction was calculated from the ac susceptibility at 5 K with a numerical correction for the demagnetization of the actual sample geometry.

3. Results and discussion

3.1 Structure, pinning and critical currents in MT-YBaCuO
Figure 1 summarizes the results on MT-YBaCuO. The structures of type 1 and 2 MT-YBaCuO are shown in figures 1a-d as obtained from optical microscopy in polarized light (polished and etched surfaces) after oxygenation at 0.1 MPa (1 atm) pressure of oxygen at 440 ^oC for 20 days (figures 1a, b) and after oxygenation at 16 MPa oxygen pressure, 800 ^oC for 3 days (figures 1c, d). Figures 1e, f, g show the whole samples after oxygenation and polishing as they look under optical microscopy in polarized light and ware composed from dozens of pictures taken one by one. Figures 1h-k present the structures obtained using transmission electron microscopy of type 1 and 2 MT-YBaCuO oxygenated under 16 MPa pressure at 650 and 800 ^oC. Figure 2 depict the j_c of MT-YBaCuO oxygenated under
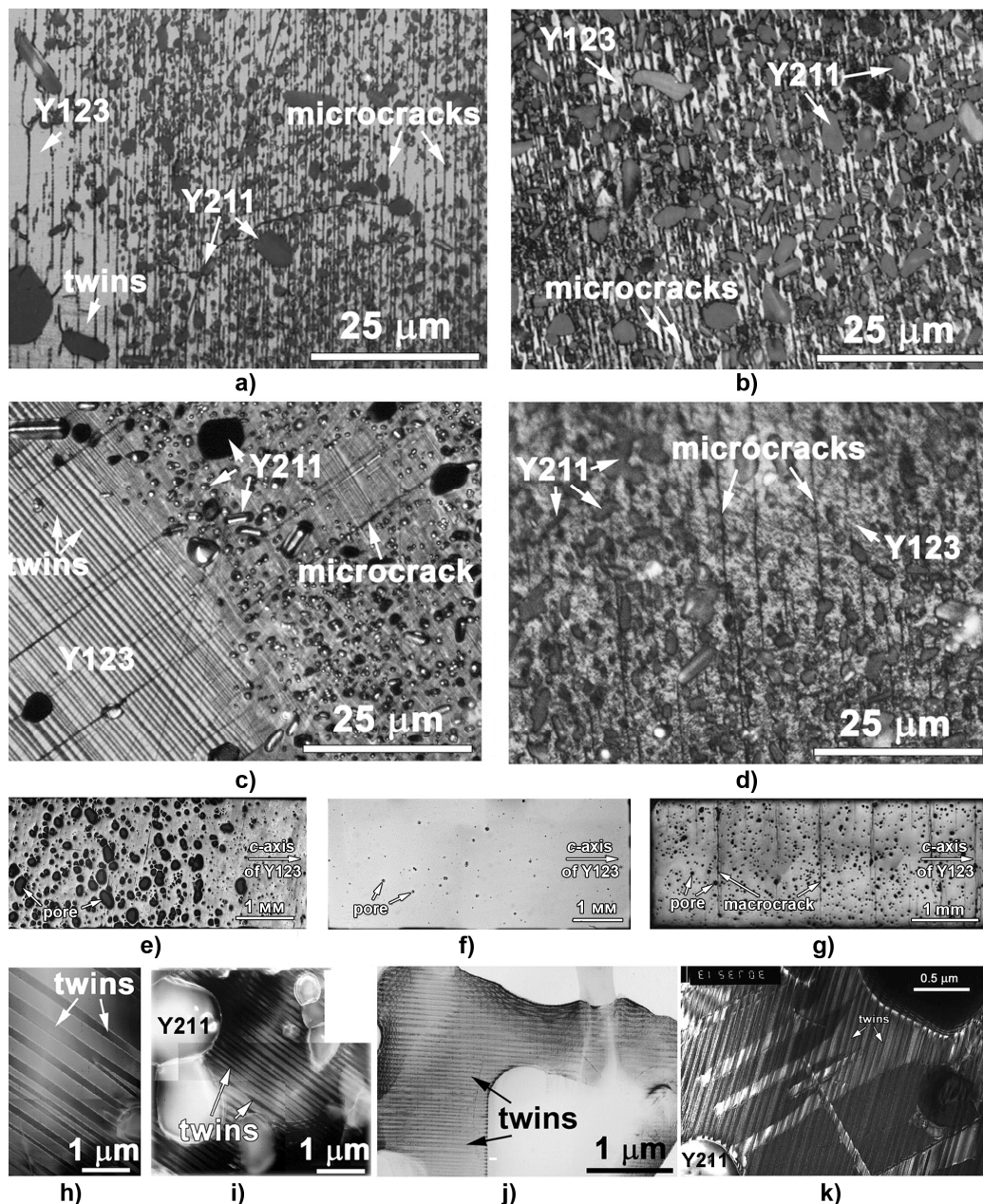
Figure 1. (a-d) − Structures of MT-YBaCuO ceramics under polarized light after oxygenation and etching: of type 1 (a, c) and type 2 (b, d), oxygenated under 0.1 MPa of oxygen at 440 °C for 20 days (a, b) and under 1–16 MPa of oxygen at 900–800 °C for 3 days (c, d); (e-k) view of the structure of MT-YBaCuO samples: (e-g) under polarized light as a whole which were used for j_c estimation (the longer side of the rectangular parallelepiped sample was parallel to the *c*-axis of Y123) and (h-k) under TEM of: (e, h, i) type 1 oxygenated under 1–16 MPa of oxygen at 900–800 °C for 3 days, (f, j) type 2 (with 0.6 mm holes) oxygenated under 1–16 MPa of oxygen at 900–800 °C for 3 days and (g, k) type 2 (traditional without holes) oxygenated under 16 MPa of oxygen at 700 °C for 3 days.

different conditions in two perpendicular directions: parallel (figure 2a, b) and perpendicular (figure 2c) to the *ab* planes. It should be mentioned that the lattice parameters of the $YBa_2Cu_3O_{7-\delta}$ phase of all MT-YBaCuO samples after oxygenation corresponded to an amount of oxygen of about 7 ($\delta \approx 0$). This means that the Y123 structure was completely oxygenated. The analysis of these results allows us to
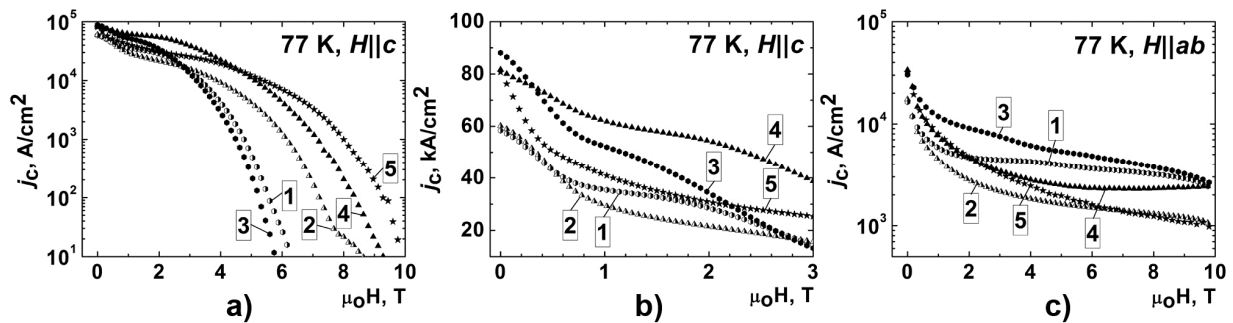
Figure 2. Critical current density, j_c, vs. magnetic field, μ_oH, at 77 K when the magnetic field was parallel to the *c*-axis of Y123 (a, b) and parallel to the *ab*-planes (c) of the MT-YBCO samples: 1, 3 – type 1 and 2, 4, 5 – type 2: 1, 2 - oxygenated under 0.1 MPa of oxygen at 440 ^{o}C for 20 days; 3, 4 – oxygenated under 1-16 MPa of oxygen at 900-800 ^{o}C for 3 days and 5 - oxygenated under 16 MPa of oxygen at 700 ^{o}C for 3 days; 1, 3, 5- traditional MT-YBaCuO without holes and 2, 4 – thin-walled MT-YBaCuO with 0.6 mm holes.

draw the following conclusions. Samples oxygenated under high oxygen pressure (16 MPa) exhibit higher critical current densities, especially in the case of type 2 MT-YBaCuO prepared from an Y123 - Y211 mixture. Comparing the structures in figures 1a-d the following differences are found. First of all, ceramics of type 1 (prepared from Y123 and Y_2O_3) have smaller and less homogeneously distributed inclusions of the Y211 phase as compared to ceramics of type 2 (prepared from Y123 and Y211). For both ceramics an essential decrease of the amount of micro-cracks parallel to the *ab*-plane was observed in the ceramic oxygenated under high oxygen pressure (factor of 4 - 4.5, i.e. from 1080-980 to 280-200 mm^{-1}), but at those places, where the distances between Y211 grains were smaller, the density of micro-cracks was much higher. The distances between Y211 in type 2 ceramics were very small and they were more homogeneously distributed, so the micro-crack density is higher than that in type 1 ceramics (factor of 1.4 for oxygenation at 16 MPa pressure). This can explain why the critical current densities of type 1 ceramics are somewhat higher (curves 1 and 3 vs. curves 2 and 4) in the direction perpendicular to the *ab*-plane (figure 2c). It should be mentioned that micro-cracks as opposed to macro-cracks can be seen in the material only after etching the polished surfaces.

The analysis of the TEM images shows the extremely high twin density in type 2 ceramics oxygenated at 650 and 800 ^{o}C under 16 MPa (figures 1j, k) and a somewhat lower density in type 1 ceramics oxygenated at 800 ^{o}C under 16 MPa (see figures 1 h, i). The twin density depends on the distribution of Y211 inclusions in Y123 as well and was higher when the distance between the Y211 inclusions was smaller. In type 1 ceramics twins can be seen even in optical microscopy in polarized light (figure 1c) at those places where the density of Y211 is low, but twins can be seen only under higher magnification at places with a high density of Y211 inclusions and small distances between them, which can be reached in transmission electron microscopes (TEM), because their density is extremely high and the twin lamella thickness is around 30-45 nm. The density of twins in high pressure oxygenated MT-YBaCuO of type 2 was about 22-35 μm^{-1} (figure 1j, k), while the ceramics of type 1 had a twin density of 4-11 μm^{-1} (in those regions, where the Y211 density was lower, a lower twin density was observed, see figures 1h, i). The densities of twins in materials oxygenated at 440 ^{o}C and 0.1 MPa were around 0.5-1.7 and 12-16 μm^{-1} for MT-YBaCuO of types 1 and 2, respectively.

It is interesting to note that high pressure oxygenation at 800 ^{o}C results in MT-YBaCuO materials, where almost only twins are present in the Y123 matrix, but no stacking faults and only very randomly located dislocations. According to the diagram of equilibrium concentration of oxygen in the Y123 structure versus the partial oxygen pressure at different temperatures by Assmus and Schmidbauer [15], full oxygenation of Y123 (7 oxygen atoms per unit cell) under 10-16 MPa pressure at such high temperature as 800 ^{o}C is impossible and 5-8 times higher pressures are necessary to keep the oxygen in Y123. But it was experimentally shown that the diffusion processes are rather quick at such temperatures and oxygen can penetrate into the Y123 structure easily, provoking just twinning and

much less cracking than in the case of lower oxygenation temperatures. An analysis of the MT-YBaCuO structure, high pressure oxygenated at 650 $^{\circ}$C (figures 1g, k), showed the presence of a lot of macro-cracks (figure 1g), 500 mm^{-1}, a very high concentration of twins (30-35 μm^{-1}) as well as stacking faults and dislocations. The high density of cracks can be an explanation for the comparatively low j_c in the direction perpendicular to the *ab*-planes (curve 5 in figure 2c). So, the temperature of 650 $^{\circ}$C was not high enough to oxygenate the material without cracking. It should be mentioned that even small samples could not be oxygenated at 440 $^{\circ}$C at least for 165 h, when an oxygen pressure of 16 MPa was applied before heating, i.e. the Y123 structure remained tetragonal and zero j_c was observed at 77 K. The oxygenation of small samples at 440 $^{\circ}$C in flowing oxygen (0.1 MPa) for 3 days gave much better results from the point of view of j_c, but it was still much lower than that of both types of samples oxygenated at 800 $^{\circ}$C and 16 MPa for the same time and their Y123 structures were partly tetragonal and partly orthorhombic.

The MT-YBaCuO materials with small holes (thin-walled ceramics) and without holes (traditional ceramics) have a different porosity (their structures are shown in figures 1f and 1g, respectively). Usually a dense layer is formed on the surfaces of traditional ceramics, while highly porous material is located below, but the thin-walled ceramics are completely dense. We studied in parallel traditional porous MT-YBaCuO ceramics prepared from a mixture of Y123 and Y211 (type 2) and conclude that porous ceramics of type 1 and type 2 behave differently concerning the amount of micro-cracks and twins because of the different distribution of Y211 particles, but not because of a difference in porosity, because the type 2 porous ceramics behave similarly to type 2 ceramics with holes. The high pressure-high temperature oxygenation (800 $^{\circ}$C, 16 MPa) allowed avoiding macro-cracking both in porous and dense MT-YBaCuO, prepared from Y123 and Y$_2$O$_3$ (type 1) and from Y123 and Y211 (type 2), see figures 1e, f.

Our experimental study showed that high critical currents were achieved in MT-YBaCuO with a high density of twins (and without dislocations and stacking faults). The authors of [4] observed an essential increase of j_c in MT-YBaCuO at low magnetic fields (below 0.3 T) after repeated oxygenation at 10 MPa and 600 $^{\circ}$C for 2-12 h of ceramics oxygenated previously at 450 $^{\circ}$C under 0.1 MPa for 120 h, but the j_c in fields above 0.3 T decreased. The increase of j_c was attributed by the authors of [4] only to the increase of dislocation density, but not to the density of twins (which increased by a factor of 1.7 as well, as our observations of the structures demonstrated). Our previous study of MT-YBaCuO samples, detwinned under high pressure (2 GPa) and having an extremely high density of dislocations (10^{12} cm^{-2}), exhibited a rather modest j_c (about 10^3 A/cm^2 in self-field). Taking all observations into consideration we come to the conclusion that in addition to the intersection places between twins pinning will occur at those places, where the twin planes cross 211 inclusions or micro-cracks and that twins play a very important role for attaining high critical currents. Usually an increase of micro-hardness and fracture toughness [17] is observed in materials oxygenated under high pressure - high temperature, which could well be the result of a decrease of the micro-crack density and an increase of the density of twins.

3.2 Structure, pinning and critical currents in MgB$_2$

Figure 3 summarizes our results on MgB$_2$ bulks and thin films. The highest j_c showed a thin MgB$_2$ film (curves 1, 2 in figures 3g, h), which contained a lot of admixed oxygen in its structure according to SEM and Auger studies. Oxygen is not uniformly distributed over the film surface (the brighter areas in figures 3e, f correspond to higher concentrations of oxygen, the surface of the film was etched by Ar ions in the chamber of the JAMP−9500F instrument before the images were taken). X-ray examinations confirmed the MgB$_2$ structure of the film. For bulk MgB$_2$ materials j_c usually increases with increasing manufacturing temperature at low magnetic fields, while j_c somewhat decreases at
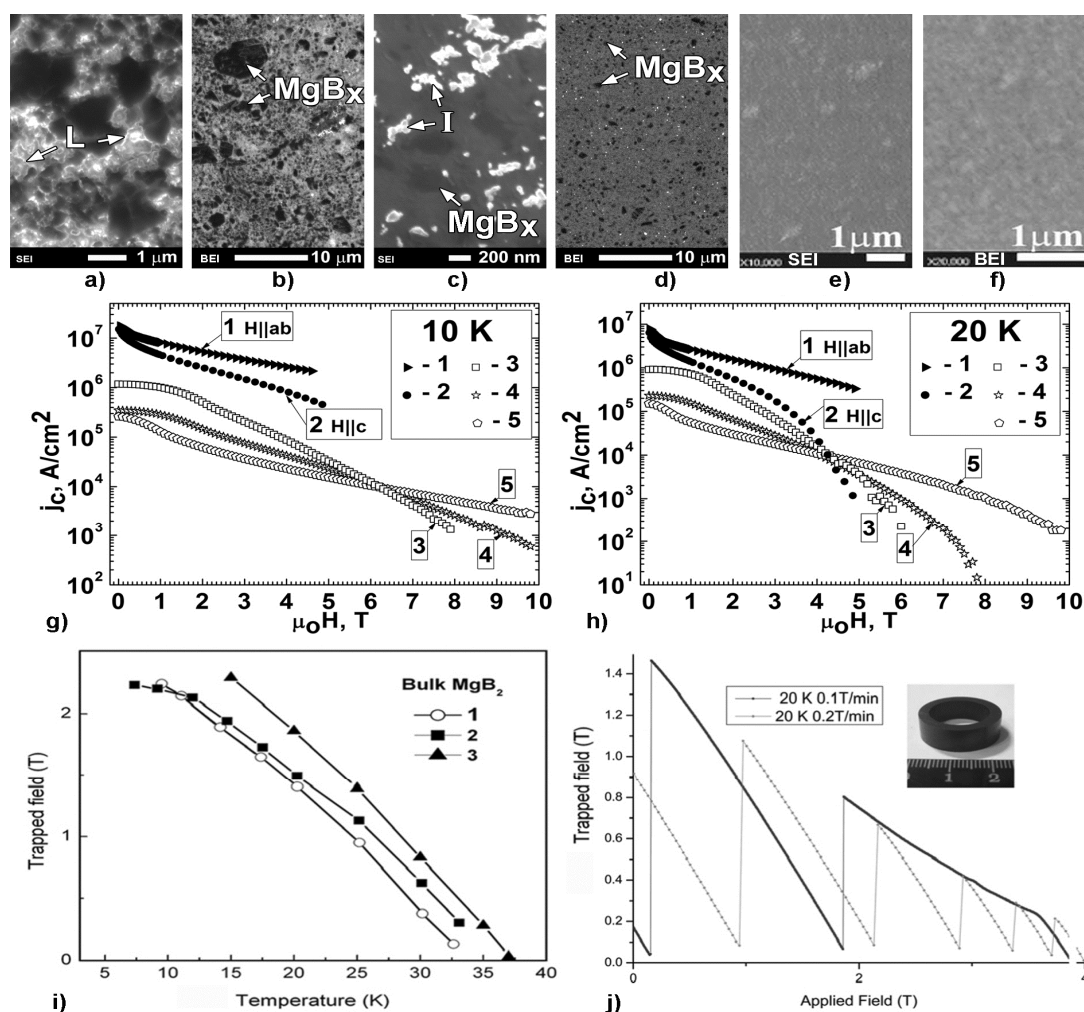
Figure 3. (a–d) - Structures of MgB$_2$ bulk (after etching by argon in the chamber of JAMP−9500F) synthesized from Mg(I):2B(I) under 2 GPa for 1 h at 800 $^{\circ}$C (a, b) and at 1050 $^{\circ}$C (c, d) in SEI (a, c) and BEI (b, d) modes ("L", "I" – Mg-B-O nano-layers and inclusions, respectively, MgB$_x$ – inclusions of higher magnesium borides x>4);

(e-f) surface of the MgB$_2$ film (140 nm thick, grown by magnetron sputtering on sapphire substrate, after etching by argon in the chamber of JAMP−9500F) in SEI (e) and BEI (f) modes (the places with higher concentration of admixed oxygen look brighter);

(g, h) – critical current density, j_c, vs. magnetic field, μ_oH, at 10 K (g) and 20 K (h) for the thin film (1, 2): (magnetic field parallel to the substrate – 1 and perpendicular – 2) and for bulks (3–5), high-pressure (2 GPa, 1 h) MgB$_2$ synthesized at: 3 - 1050 $^{\circ}$C from Mg(I):2B(I), 4 - 800 $^{\circ}$C from Mg(I):2B(I) and 5 - 600 $^{\circ}$C from Mg(I):2B(II);

(i) - trapped fields at the sample centre of MgB$_2$ blocks of different sizes: 1 - 14×14×4 mm^3 (from Mg(I):2B(IV) with 10% Ti), 2 - 22.5 mm in diameter and 6 mm in height (from Mg(I):2B(IV) with 5% of Ta), 3 - 30 mm in diameter and 7.5 mm in height (from Mg(I):2B(III) with 10% Ti);

(j) trapped field at 20 K at the center of the MgB$_2$ ring from Mg(I):2B(III) with 10% SiC (Ø24.3×17.9 mm, h=7.8 mm, see upper right insert). The measurements were performed with different sweep rates of the external magnetic field (0.1 T/min: solid line, 0.2 T/min: gray line with squares).

high magnetic fields (curves 3-5 in figures 3g, h), which is accompanied by a transformation of Mg-B-O nanolayers into separate Mg-B-O inclusions (the brightest areas in figures 3a, c) and by a reduction of MgB$_x$ (x >4 and usually x=10-14 for materials prepared at 2 GPa; darkest areas in figures 3d, c).

Comparing the structures and characteristics of MgB_2 we conclude that the most important role for pinning is played by the distribution of admixed oxygen in the structure and that its generally high amount (5-17 wt%) is certainly not an obstacle for very good superconducting characteristics (figures 3g - 3j). MgB_2 bulks manufactured under 30 MPa – 2 GPa pressure showed 73-98 % connectivity and 75-100 % shielding fraction. We did not observe MgO by SEM and Auger techniques. The presence of some (5-13 wt%) MgO in the x-ray diffraction pattern makes us assume that the brightest Mg-B-O areas represent solid solutions of boron in the MgO structure (up to about MgBO level). Our careful Auger study [14] showed that some oxygen is solved in the MgB_2 matrix as well ($MgB_{2.2-1.7}O_{0.4-0.6}$ according to a quantitative Auger analysis). Calculations of the density of electronic states (DOS) and of the binding energy, E_b, (Table 2) confirmed that, from the point of view of carrier concentration near the Fermi level (metallic-like behaviour) and the similarity of the binding energy with that of MgB_2, the excellent superconducting performance of the $MgB_{1.5}O_{0.5}$ compound does not contradict theoretical predictions. To calculate the DOS and E_b we applied the density functional theory [18] based on a full-potential linearized augmented plane wave method with the generalized gradient correction to the exchange-correlation potential [19] using WIEN2k [20].

Table 2. Total DOSs and binding energies, E_b, in the $Mg(B_{1-x}O_x)_2$ compounds.

x	0	0.125	0.25	0.5
total DOS	0.72	0.43	0.96	1.36
E_b, Ry	1.12	1.10	1.06	0.94

3.3 Trapped fields of MT-YBaCuO and MgB₂ bulk
The trapped magnetic field is one of the most comprehensive characteristics of superconducting ceramics from the point of view of perspectives for their application. The strength of the magnetic field of a magnetized bulk depends on the material's j_c and its volume. Therefore, the size, homogeneity and perfection of the bulk structure play a very important role. The trapped field distribution (field mapping) is assessed by scanning the surface using Hall probes and represents the main characterization technique for MT-YBaCuO bulks. MT-YBaCuO blocks of $38\times38\times17$ mm^3 (type 1) oxygenated at 440 ^{o}C and 0.1 MPa for 20 days trapped a maximal field of 1.44 T at 77 K. MT-YBaCuO (type 2) with 16 mm in diameter, 10 mm thick, and with 0.6 mm holes trapped a maximal field of 0.65 T after oxygenation at 800 ^{o}C and 16 MPa for 3 days and just 0.24 T after oxygenation at 0.1 MPa and 420-390 ^{o}C for 18 days. MT-YBaCuO (type 2) with 16 mm in diameter, 10 mm thick, and with 0.45 mm holes trapped a field of 0.84 T after oxygenation at 800 ^{o}C and 10 MPa for 53 h.

In the case of MgB_2 the working temperature is rather low and the scanning devices at such low temperatures (20 K) are rather scarce. Therefore, trapped fields of MgB_2 are often estimated from only one point (in the middle of the top surface of the bulk, where the highest trapped field value is expected). The temperature dependence of trapped fields of MgB_2 is shown in figure 3i. MgB_2 is very sensitive to flux jumps and, as shown in figure 3j, the trapped field in MgB_2 depends to a high extent on the speed of the external magnetic field variation. This makes a pulsed magnetization of MgB_2 extremely difficult and restricts applications under ac current conditions. We succeeded to trap 1.8 T at 20 K (figure 3i) in the middle of an MgB_2 block of 30 mm in diameter, 7.5 mm thick.

4. Conclusions

The investigation of the oxygenation process of MT-YBCO ceramics with different sizes and distributions of Y211 particles in the Y123 structure allowed us to conclude that twins influence pinning and thus the critical current density at elevated temperatures to a high extent, but their density as well as the density of micro-cracks parallel to the *ab*-plane depend to a high extent on the distances between Y211 inclusions. Both the density of twins and of micro-cracks increases with a reduction of these distances. Oxygenation under elevated oxygen pressure (10-16 MPa) and at high temperature (800 ^{o}C) allows to increase j_c and the trapped field, which is, as we assume, due to the enhancement of the diffusion processes and an oxygenation of the Y123 structure under softer conditions in much

shorter times leading to an essential increase in twin density and a reduction of micro-cracking. Pinning in MgB_2 depends to a high extent on the distribution of admixed oxygen, which can be influenced, e.g., by the synthesis temperature. The relevant pinning centers are in our opinion nano-areas of solid solutions of boron in MgO (up to the MgBO level) and inclusions of higher magnesium borides MgB_x (x>4), the sizes and distribution of which also depend on the synthesis conditions. The dissolved oxygen in the MgB_2 structure does not depress superconductivity in MgB_2 also from the point of view of DOS and binding energy. The level of the trapped magnetic fields depends in MgB_2 to a high extent on the rate of the external magnetic field variation.

References

[1] Prikhna T, Eisterer M, Gawalek W et al. 2015, *Superconductors and Superconductivity. Specialized Collections* **4** 30.

[2] Prikhna T, Noudem J, Gawalek W et al. 2012, *Materials Science Forum* **721** 3.

[3] Yamamoto A, Ishihara A, Tomita M and Kishio, K 2014 *Applied Physics Letters* **105** 032601.

[4] Plain J, Puig T, Sandiumenge F, Obradors X and Rabier J 2002 *Physical Review B* **65** 104526.

[5] Takizawa T and Murakami M 2005 Critical Currents in Superconductors, Editor M. Murakami Tokyo: Nihon University College of Humanities and Sciences.

[6] Gawalek W, Habisreuther T, Zeisberger M, Litzkendorf D, Surzhenko O, Kracunovska S, Prikhna T A, Oswald B, Kovalev L K and Canders W 2004 *Supercond. Sci. Technol.* **17** 1185.

[7] Deng Z, Izumi M, Miki M, Tsuzuki K, Felder B, Liu W, Zheng J, Wang S, Wang J, Floegel-Delor U, Werfel F N 2012 *IEEE Transactions on Applied Superconductivity* **22,** 2, 6800210.

[8] Murakami M 1993 Melt processed high-temperature superconductors, Editor Murakami M World Scientific: Singapore-New Jersey – London - Hon-Kong 380.

[9] Diko P 2004 *Supercond. Sci. Technol.* **17** 45.

[10] Boyko V S, Siu-Wai Chan 2007 *Physica C* **466** 56.

[11] Liao X Z, Serquis A C, Zhu Y T, Huang J Y, Civale L, Peterson D E, Mueller F M and Xu H 2003 *Journal of Applied Physics* **93** 6208.

[12] Prikhna T A, Eisterer M, Weber H W, Gawalek W, Kovylaev V V, Karpets M V, Basyuk T V and Moshchil V E 2014 *Supercond. Sci. Technol.* **27**, No 4 044013.

[13] Birajdar B, Braccini V, Tumino A, WenzeT, Eibl O and Grasso G 2006 *Supercond. Sci. Technol.* **19** 916.

[14] Muralidhar M, Sakai N, Chikumoto N, Jirsa M, Machi T, Nishiyama M, Wu Y, Murakami M 2002, *Phys. Rev. Lett.* **89,** No 23 237001_1.

[15] Assmus W, Schmidbauer W 1993 *Supercond. Sci. Technol.* **8** 555.

[16] Chaud X, Bourgault D, Chateigner D, Dico P, Porcar L, Villaume A, Sulpice A, Tournier R *Supercond. Sci. Technol.* 2006 **19** S590.

[17] Prikhna T, Chaud X, Gawalek W, Rabier J, Savchuk Y, Joulain A, Vlasenko A, Moshchil V, Sergienko N, Dub S, Melnikov V, Litzkendorf D, Habisreuther T, Sverdun V 2007 *Physica C* **460-462** 392.

[18] Parr R G and Yang W 1989 Density-Functional Theory of Atoms and Molecules, *Oxford Univ. Press*.

[19] Perdew J P, Burke S and Ernzerhof M 1996 *Phys. Rev. Lett.* **77** 3865

[20] Blaha P, Schwarz K, Madsen G K H, Kvasnicka D, and Luitz J 2001 WIEN2K, An augmented plane wave + local orbitals program for calculating crystal properties. *Techn. Univ. Wien*.